Definition and Inspection of Profile and Lead of a Worm Wheel

Dr. Donald R. Houser and Dr. Xiaogen Su

Introduction

Traditionally, profile and lead inspections have been indispensable portions of a standard inspection of an involute gear. This also holds true for the worm of a worm gear drive (Ref. 1). But the inspection of the profile and the lead is rarely performed on a worm wheel. One of the main reasons is our inability to make good definitions of these two elements (profile and lead) for the worm wheel. Several researchers have proposed methods for profile and lead inspections of a worm wheel using CNC machines or regular involute measuring machines. Hu and Pennell measured a worm wheel's profile in an "involute" section and the lead on the "pitch" cylinder (Ref. 2). This method is applicable to a convolute helicoid worm drive with a crossing angle of 90° because the wheel profile in one of the offset axial planes is rectilinear. This straight profile generates an involute on the generated worm wheel. Unfortunately, because of the hob oversize, the crossing angle between the hob and the worm wheel always deviates from 90° by the swivel angle. Thus, this method can be implemented only approximately by ignoring the swivel angle. Another shortcoming of this method is that there is only one profile and one lead on each flank. If the scanned points deviate from this curve, it produces unreal profile deviation. Octrue discussed profile inspection using a profile checking machine (Ref. 3).

If the swivel angle is not ignored, the involute profile used in Reference 2 does not exist, and the profile equation developed in Reference 3 does not apply. Thus, profile and lead inspection is not often performed to qualify a worm wheel. To verify the compatibility of the wheel tooth with that of a mating worm, the wheel is assembled with a master worm on a test rig and a rolling test is performed (Ref. 1). The contact pattern developed by painting the worm is used to judge the quality. This kind of rolling test works well in terms of functionality, but it does not give enough quantitative data to the designer and the hobbing machine operator. In other words, the rolling test results cannot be fully used for quality improvement.

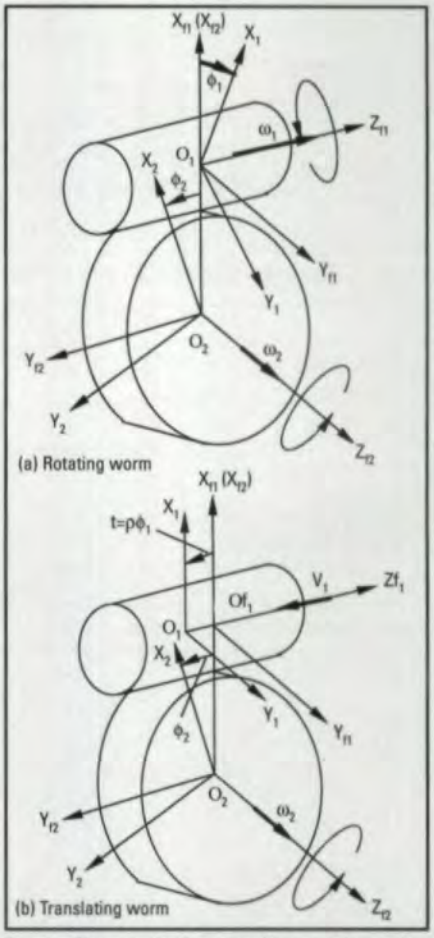

Fig. 1—Two equivalent meshing motions of a worm gear drive.

NOMENCLATURE

E	Center distance between the hob/worm axis and the wheel axis while meshing
X_1	$= [x_1, y_1, z_1]^T$, worm surface point vector
X_2	$= [x_2, y_2, z_2]^T$, wheel tooth surface point vector
m_{21}	The gear ratio (number of worm threads / number of wheel teeth)
n_1	$= [n_{x1}, n_{y1}, n_{z1}]^T$, normal vector at a worm surface point
t	$= -\rho\phi_1$, equivalent translation displacement of the worm
u	Surface parameter on the worm thread in radial direction
v_i^{12}	The relative velocity between part 1 (hob/worm) and part 2 (wheel) while meshing
α	Profile angle of the grinder
γ	Crossing angle between the worm axis and the wheel axis while meshing
ϕ_1	The worm rotation angle while meshing
θ	Surface parameter on the worm thread in circumferential direction
ρ	Screw parameter of the hob/worm, equal to the lead divided by 2π

Dr. Donald R. Houser
is director of both the Center of Automotive Research and the Gear Dynamics and Gear Noise Research Laboratory at Ohio State University. His research is directed toward the reduction of gear noise through modification to the gear tooth surface design. Research is also oriented toward the measurement of dynamic and static transmission error of gears as well as automotive noise measurements for sound quality evaluation.

Dr. Xiaogen Su
received his doctorate from Ohio State University in June 1999. His principal area of research is gear inspection and reverse engineering. He worked as an engineer and teacher for seven years before coming to the U.S. and now is employed in China by the Copeland Corporation.

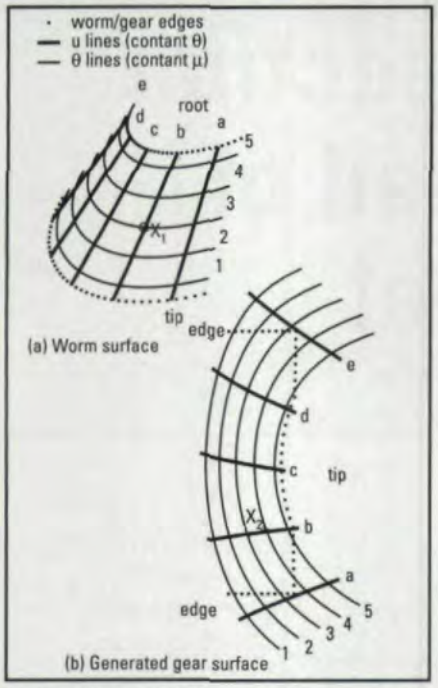

Fig. 2—*u* lines and *θ* lines of a ZK worm wheel.

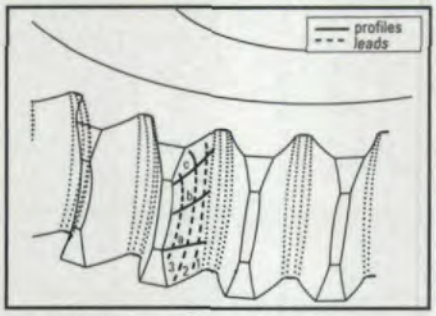

Fig. 3—Multiple profiles and leads.

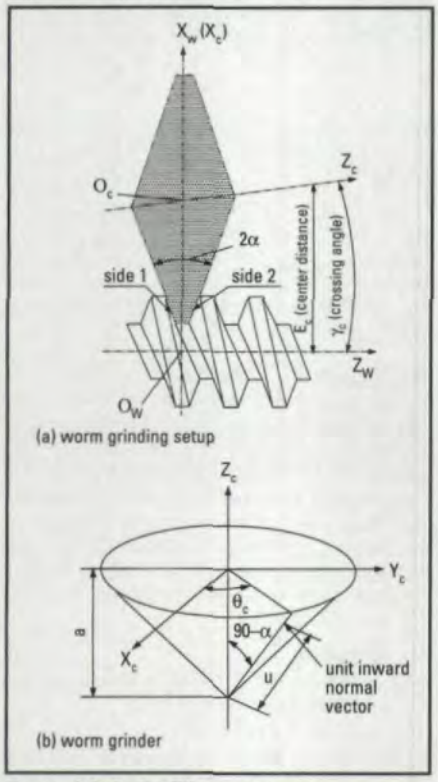

Fig. 4—Grinder for ZK-type of worm.

In this article, an explicit equation of the generated wheel tooth is derived. This equation applies to any type of single enveloping worm gearing. The crossing angle between the hob/worm axis and the wheel axis is not limited to 90°. Thus, this equation can also be used for non-right-angle worm gearing. Based on the explicit tooth equation, profiles and leads of a worm wheel are redefined. The new definitions are comparable to their counterparts of an involute gear. There are an infinite number of profiles (at different "face positions") and leads (at different "diameters"), as there are on an involute gear. All of the profile and lead curves can be expressed explicitly and can be readily measured by a CNC measuring machine. Inspection examples are given (a CMM is used for the measurement) to illustrate the application.

Explicit Expression of the Generated Worm Wheel Tooth

The geometry of a generated worm wheel is very complex. An explicit equation of the wheel tooth surface has not been found before. The traditional expression of the generated worm wheel tooth, as presented in Reference 4, is in the form of:

$$X = X\,(u, \theta, \phi_1) \qquad (1)$$

$$\text{Subject to } f\,(u, \theta, \phi_1) = 0 \qquad (2)$$

The constraint $f = (u, \theta, \phi_1)$ is the equation of meshing for cutting. The commonly used equation of meshing for worm gear drives was proposed by Litvin (Ref. 5). It is:

$$(z_1\cos\phi_1 + E\cot\gamma\sin\phi_1)\,n_{x1} + (-z_1\sin\phi_1 + E\cot\gamma\cos\phi_1)\,n_{y1} - \left[(x_1\cos\phi_1 - y_1\sin\phi_1 + E) - \rho\,\frac{1\text{-}m_{21}\cos\gamma}{m_{21}\sin\gamma}\right] n_{z1} = 0 \quad (3)$$

where $X_1 = [x_1, y_1, z_1]^T$ is the surface point vector and $n_1 = [n_{x1}, n_{y1}, n_{z1}]^T$ is the corresponding normal vector of the worm thread surface in a coordinate system attached to the worm itself (See Fig. 1). The expression $X_1 = X_1\,(u, \theta)$ of the worm thread of various types of single enveloping worm gear drives can be found in Reference 5.

Equation 3 has three parameters: u, θ and ϕ_1. Here u and θ are the two surface parameters of the meshing worm surface and variable ϕ_1 is the meshing parameter (the worm rotation angle in this equation). It is difficult to explicitly express any variable among u, θ and ϕ_1 in terms of the other two. With this equation of meshing, each point on the wheel tooth is associated with three variables that are constrained by the meshing equation (Eq. 3). This brings much inconvenience when performing surface description and surface computation (Ref. 6).

Our new expression for the generated worm wheel tooth is made possible with a new equation of meshing for worm gear drives. The new equation of meshing is based on an observation that *the rotation of the worm about its axis may be kinematically replaced by a translation along its axis* (See Fig. 1b). The relation between the rotation angle ϕ_1 and the translation t is

$$t = -\,\rho\phi_1 \qquad (4)$$

We will derive the equation of meshing with the translating meshing motion. The general equation of meshing for all types of gearing is

$$n_i \bullet v_i^{12} = 0 \qquad (5)$$

where i represents the coordinate system. For convenience, the fixed coordinate system S_{f1} (shown in Fig. 1b) is used. Coordinate system S_{f1} coincides with the coordinate system S_1 attached to the worm when the worm has zero translation. In coordinate system S_1,

$$X_1 = [x_1, y_1, z_1]^T \qquad (6)$$

$$n_1 = [n_{x1}, n_{y1}, n_{z1}]^T \qquad (7)$$

From Figure 1, the same point and its normal can be expressed in coordinate system S_{f1} as

$$X_{f1} = [x_{f1}, y_{f1}, z_{f1}]^T = [x_1, y_1, z_1 - \rho\phi_1]^T \quad (8)$$

$$n_{f1} = [n_{xf1}, n_{yf1}, n_{zf1}]^T = [n_{x1}, n_{y1}, n_{z1}]^T \quad (9)$$

The relative velocity at the meshing point in coordinate system S_{f1} is $v_{f1}^{12} = v_{f1}^{1} - v_{f1}^{2}$, and

$v_{f1}^{1} = [0, 0, -\rho\phi_1']^T$

$$v_{f1}^{2} = \begin{vmatrix} i & j & k \\ 0 & m_{21}\,\phi'_1 \sin\gamma & m_{21}\phi'_1 \cos\gamma \\ x_1+E & y_1 & z_1 - \rho\phi_1 \end{vmatrix}$$

$$v_{f1}^{12} = -\,m_{21}\phi'_1 \begin{vmatrix} (z_1 - \rho\phi_1)\sin\gamma - y_1\cos\gamma \\ (x_1 + E)\cos\gamma \\ \rho/m_{21} - (x_1 + E)\sin\gamma \end{vmatrix} \tag{10}$$

From equations 5, 9 and 10, we get the alternative equation of meshing:

$$[(z_1 - \rho\phi_1)\sin\gamma - y_1\cos\gamma]\, n_{x1} + (x_1 + E)\cos\gamma n_{y1} + [\rho/m_{21} - (x_1 + E)\sin\gamma]\, n_{z1} = 0 \tag{11}$$

Thus, the meshing parameter ϕ_1 can be expressed explicitly by the two surface parameters, u and θ, of the generating surface as

$$\phi_1 = \frac{(x_1 + E)\cot\gamma n_{y1} + (\rho/m_{21}/\sin\gamma - (x_1 + E))\, n_{z1} + (z_1 - y_1\cot\gamma)\, n_{x1}}{\rho n_{x1}} \tag{12}$$

Through transformations, in the coordinate system S_2, attached to the wheel itself, the generated wheel tooth surface X_2 can be expressed as

$$\begin{aligned} X_2 &= R_z[-m_{21}\phi_1(u,\theta)]T_x(E)R_x(\gamma) \\ &\quad T_z(-\rho\phi_1(u,\theta))X_1(u,\theta) \\ &= X_2(u,\theta) \end{aligned} \tag{13}$$

where $X_1(u, \theta)$ is the hob/worm thread surface expressed in the coordinate system S_1 attached to the hob/worm itself. The matrix $T_i(t)$ defines a translation of distance t along axis i, and the matrix $R_i(r)$ defines a rotation by an angle of r about axis i.

In this way, u and θ can be treated as two surface parameters of both the worm thread surface and the generated wheel tooth surface. Parameter θ is the rotation angle of the screw motion to form the hob/worm thread, and parameter u may have different physical meaning for different types of worm gearing. Equations 12 and 13 define a mapping point X_1 of the worm surface into point X_2 on the generated wheel tooth. A pair of lines (u, θ) specifies one point on the worm thread surface and its corresponding point on the generated wheel tooth. Figure 2a shows the u lines and θ lines on the surface of a worm thread. Figure 2b shows the corresponding u lines and θ lines on the surface of the wheel tooth generated by this worm.

The explicit expression of $X_2 = X_2(u, \theta)$ is significant. It reduces the level of complexity of the generated worm wheel tooth surface to that of a surface with analytical accessibility similar to that available for involute spur or helical gear teeth.

The same idea can be readily extended to the analysis of helicon gearing (Ref. 7) and the hobbing process. In helicon gearing, the pinion is actually a worm, and its rotation can be replaced by a translation along its axis to reduce the complexity of the kinematic analysis.

Definitions of Profile and Lead of a Worm Wheel

As with spur and helical gears, we desire definitions of profiles and leads

that allow them to be defined at multiple locations across the tooth surface. For an involute spur/helical gear, the tooth surface can be written as:

$$X = X(\epsilon, f) \tag{14}$$

where ϵ is the roll angle and f is the face position parameter. A pair (ϵ, f) determines a point and its normal on a certain tooth flank. The defined profiles and leads of the involute gear correspond to the ϵ lines and the f lines, respectively. If the parameter f is fixed at f_0, the curve $X = X(\epsilon, f_0)$ represents a profile of the gear at face position f_0; if the parameter ϵ is fixed at ϵ_0, the curve $X = X(\epsilon_0, f)$ represents a lead of the gear at roll angle ϵ_0.

An equation (13) of the generated worm wheel tooth similar to Equation 14 for the tooth of an involute gear has been developed:

$$X_2 = X_2\,(u, \theta) \tag{15}$$

Here, we define the profiles and the leads of a worm wheel in a format similar to that used for an involute gear. From Equation 15, if the parameter θ is fixed at θ_0, the curve $X_2 = X_2\,(u, \theta_0)$ traced out by changing u is defined as a profile of the worm wheel tooth; if the parameter u is fixed at u_0, the curve $X_2 = X_2\,(u_0, \theta)$ traced out by changing θ is defined as a lead. The profiles and the leads defined in this way have explicit mathematical expressions, so the profiles and the leads can be programmed and measured with CNC measuring machines.

The profile defined by $X_2(u, \theta_0)$ is not a planar curve. It runs across the tooth surface from the root area to the tip area, and this profile is called a profile at parameter θ_0. The lead defined by $X_2(u_0, \theta)$ does not lie on one cylindrical surface. It runs across the tooth surface from one edge to the other, and this lead is called a lead at parameter u_0. There are an infinite number of profiles and leads on each flank (Fig. 3). Any surface point is the intersection between a profile and a lead, and there is one profile and one lead passing through the pitch point of the worm wheel.

Take ZK-type of worm gearing as an example. A ZK-type of worm is ground by a biconical grinder (Ref. 5), as shown in Figure 4. Parameter u is the distance from the apex of the cone to a point on the grinder profile. The u lines (profiles) and the θ lines (leads) on the hob/worm thread and the generated worm wheel are plotted as in Figure 2. In this case, the hob/worm profile is not the axial section of the hob/worm thread. It is the tangency line between the hob/worm grinder and the hob/worm thread. The hob/worm lead is the helix line. Because of the one-to-one mapping of points on the hob/worm thread to the points on the worm wheel tooth defined by Equation 13, a hob/worm profile generates a wheel profile, and a hob/worm lead generates a worm wheel lead. Obviously, the profile deviation and the lead deviation measured on the wheel directly reflect the errors of the hob and the hobbing settings. Thus, the inspection results can be

more efficiently used for later quality improvement.

Figure 5 shows the profiles (u lines) and the leads (θ lines) of a ZA-type of worm gearing. In this case, the hob/worm profile is the axial section of the hob/worm thread, and the physical meaning of the parameter u is shown in Figure 6.

Inspection of Profile, Lead and Topography

The profiles and leads defined above have explicit equations, and a CNC measuring machine can be programmed to follow a profile/lead trace. For the purpose of inspection, the measured traces are compared with their theoretical position to produce the deviation charts. The deviation chart of the profile $X_2(u, \theta_0)$ is plotted against the parameter u, and the deviation chart of the lead $X_2(u_0, \theta)$ is plotted against the parameter θ.

There are two ways to perform the inspection of a wheel. First, the worm wheel can be inspected against the meshing process (the worm design and the meshing setup). The actual wheel tooth surface is compared with a virtual wheel, which is conjugate to the worm part. Large surface deviations are expected because of the difference between the hob and the worm. The deviation of the profile tells the amount of tip relief and root relief, while the deviation of the lead reveals end relief introduced by the hob oversize. Second, the wheel can be inspected against the hobbing process (the hob design and the hobbing setup). The deviation caused by the difference between the hob and the worm part will not show up as surface deviation. Because the hob shape changes due to resharpening and/or wear, the design dimensions of the hob are used. The measured deviation would now reveal the difference introduced by the decrease of the hob oversize. Very likely, the lead has a negative crowning rather than positive. This inspection may give a good idea on how the resharpening process affects the worm wheel surface.

A topographical chart can be obtained if a grid is made of points formed by profiles at different "face positions" and leads at different "diameters." Two different presentations can be used: the chart is plotted over a grid of parameter-u x parameter-θ or plotted over a grid of radius x face position.

Example of Worm Wheel Inspection

A 30-tooth, ZK-type worm wheel was inspected. The measured wheel tooth was compared with a virtual wheel tooth conjugate to the mating worm. Figure 7 shows profile traces for both sides of four separate teeth. The inspected teeth are the 1st, 8th, 16th and 23rd ones. The root relief shows up clearly, but the left flank has less tip relief than the right flank. A possible reason for this is nonsymmetry of the hob grinder, but it may come from totally different aspects, such as an orientation error of the wheel.

Figure 8 shows lead traces for both sides of the same four teeth. The end relief introduced by hob oversize is considerable. With the decrease of hob oversize, the amount of the end relief is expected to decrease. The swivel angle adopted for wheel hobbing has a direct impact on the slope of the lead. The accuracy of the middle face position may affect the slope of the lead trace. This accuracy is discussed in the next section.

Figure 9 and Figure 10 show the multiple profile and lead traces of one tooth of the same wheel. The profile traces were measured at three different θ values ("face positions"), and the leads were measured at three different u values ("diameters"). Different profile/lead traces may have different numbers of recorded points when the same increment of u/θ is used for the measurements because of the shape of the wheel tooth and the distortion of the mapping defined by Equation 13. As in the case of an involute gear inspection, the profile/lead traces on the same tooth at different locations should follow the same shape. In our inspection, it is found that the lead traces are quite similar to each other, while the profile traces differ from one another. We believe this is due to cutting scallops. These scallops create waviness on a profile trace, and the waviness shows up with different phases at different inspection positions. The effect of the

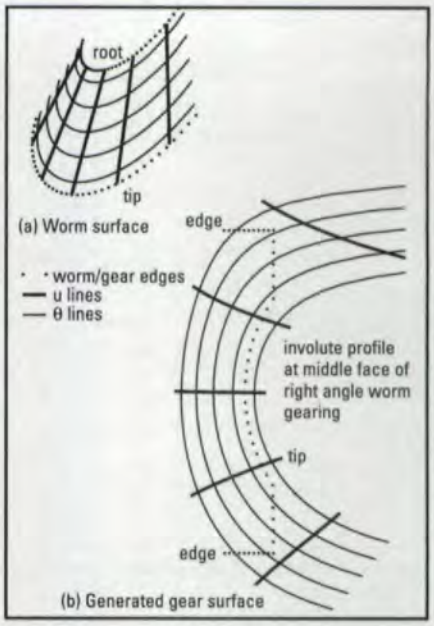

Fig. 5—Profiles (u lines) and leads (θ lines) of a ZA worm wheel.

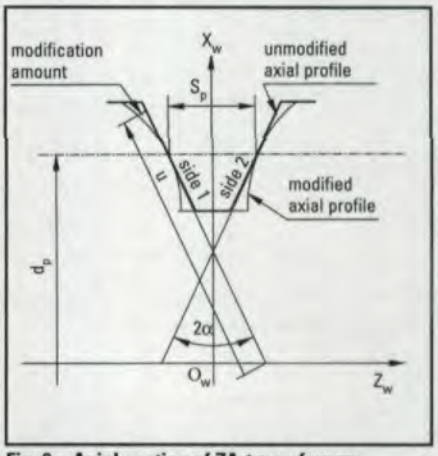

Fig. 6—Axial section of ZA-type of worm.

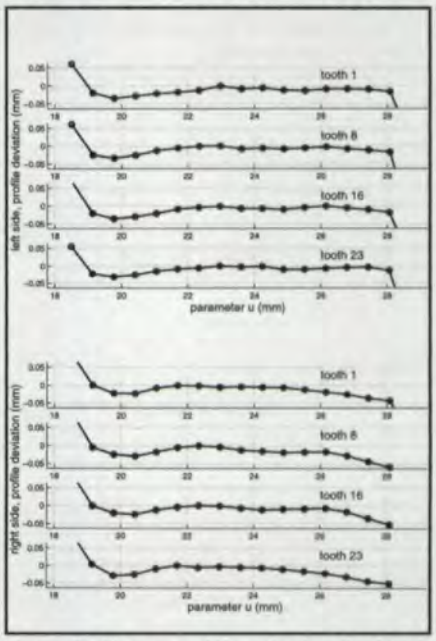

Fig. 7—Profile traces of four wheel teeth at "middle face position."

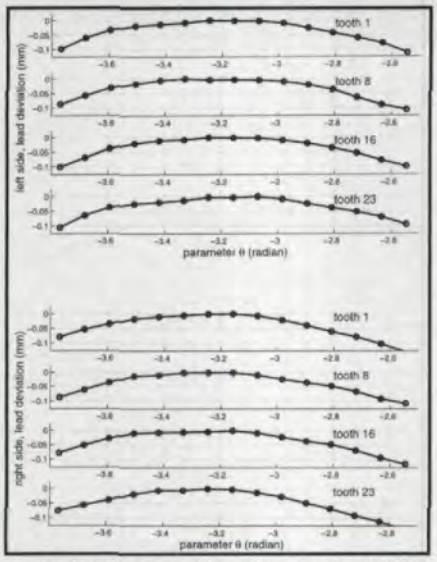

Fig. 8—Lead traces of four wheel teeth at "pitch diameter."

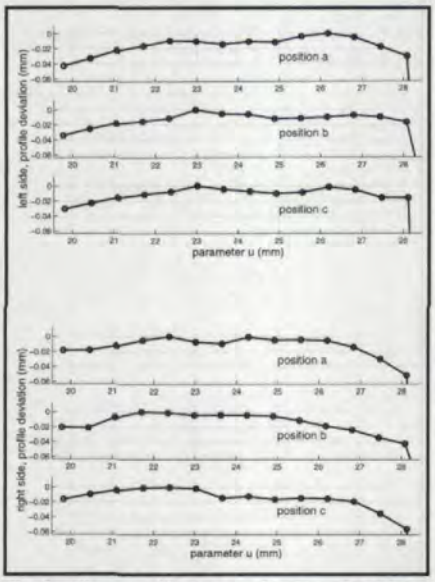

Fig. 9—Three profile traces of one tooth at three different "face positions."

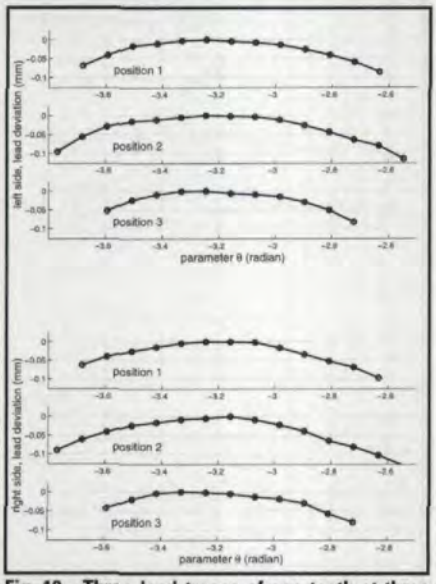

Fig. 10—Three lead traces of one tooth at three different "diameters."

scallops on the lead traces is not as large as that on the profile traces partly because the scallops run along the lead direction.

Figure 11 shows the topographical chart of the left flank of the first tooth. In total, 936 points were measured. The points are the intersection points between 40 leads (θ lines) and 30 profiles (u lines). In Figure 11a, the topographical deviation is plotted over a u x θ grid, and in Figure 11b, the topographical deviation is plotted on a R x F grid. (R is the radius of the measured point, and F is its face position.) In Figure 11b, the points with a deviation of –0.0254 mm are also drawn. The shape formed by these points can be related to the contact pattern.

Measurement Reference Frame

One very important issue for the measurement and inspection of a worm wheel is the establishment of the reference frame. There are four types of reference misalignments: eccentricity, wobble, the middle face datum and the orientation of the teeth. Each of these misalignments affects the inspection results. As usual, the Z axis of the bore (or the shaft) is used as the wheel axis. To define the middle face datum, one end face position can be used, and the distance from the middle face datum to this end face must be strictly controlled during hobbing. The orientation of the wheel can be defined by a center direction of a tooth or the center direction of a tooth space. This can only be achieved by measuring points on two tooth flanks.

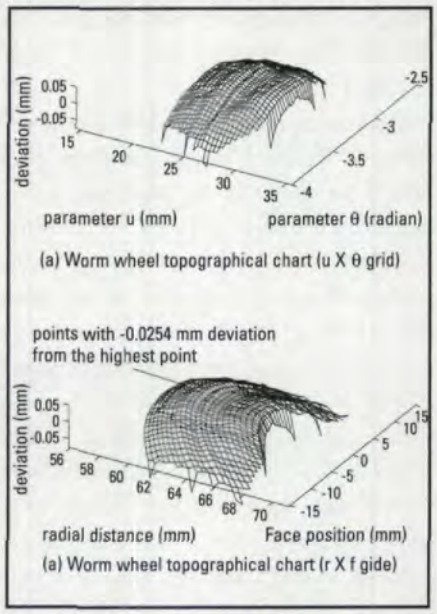

Fig. 11—Topographical inspection of a worm wheel tooth.

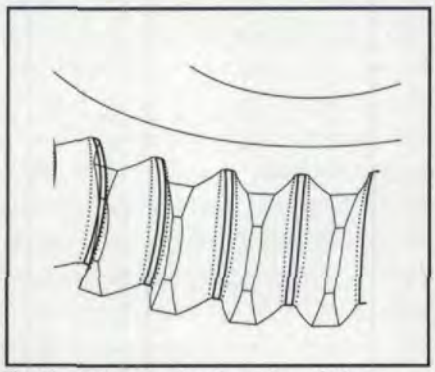

Fig. 12—Bottom land surface of revolution.

The effect of eccentricity and wobble on profile and lead inspection is similar to that of the inspection of an involute gear. A middle face datum misalignment introduces slopes on lead traces; the leads of the left side and the right side of one tooth tilt in different directions. The wheel orientation misalignment introduces slopes of profile traces, and the slopes of the left profile and the right profile have different directions.

To achieve a good middle face datum, *the authors used the measurement data of* the bottom land surface of revolution (see Fig. 12). The bottom land surface of revolution consists of all of the bottom lands between two consecutive teeth. Its shape is determined by three parameters: the hobbing center distance, the radius of the top cylinder of the hob and the amount of the swivel angle. This surface of revolution is symmetrical to the wheel's middle face position. If this surface is measured, surface fitting produces a very good middle face datum. *There are two restrictions* to apply this method: (1) the top blade of the hob must be straight; (2) the bottom land surface must be large enough for probe access.

Summary

In this article, we have presented new definitions of profiles and leads of a worm wheel based on an explicit equation of the generated wheel tooth surface. The new definitions are comparable to their counterparts of an involute gear. *Then, the inspection of profile, lead and* topography is discussed. Two methods of inspecting profiles and leads are proposed, and an inspection example of a

ZK-type worm wheel is given. The procedure to define a good reference frame for worm wheel inspection is also discussed. The explicit equation of the generated wheel tooth surface derived in this article applies to both right-axis and non-right-angle worm gearing.

Acknowledgment

The authors would like to thank the sponsors of the Gear Dynamics and Gear Noise Research Laboratory at The Ohio State University for their encouragement and financial support of the research discussed in this article.

References

1. Barber, C. "Worm Gear Measurement." *Gear Technology*, September/October 1997.
2. Hu, J. and J.A. Pennell. "A Practical Method of Measuring the Worm Wheels of Cylindrical Worm Gears." *Proceedings of the 1994 International Gearing Conference*, I. Mech. E., New Castle, England.
3. Octrue, M, M. Denis and L. Faure. "How to Inspect the Profile of a Worm Gear." *Proceedings of the 1984 ASME Design Engineering Technical Conference*, Paper No. 84–DET-204.
4. Litvin, F.L. and V. Kin. "Computerized Simulation of Meshing, Bearing Contact for Single Enveloping Worm Drives." *Journal of Mechanical Design*, Vol. 114, pp. 313–316.
5. Litvin, F.L. *Gear Geometry and Applied Theory*. PTR Prentice Hall, 1994, pp. 11–117.
6. Su, X. and D.R. Houser. "Coordinate Measurement and Reverse Engineering of ZK Type Worm Gearing." *Proceedings of 1997 AGMA Fall Technical Meeting*, Paper No. 97FTMS1.
7. *ITW Design Manual No. 6, Spiroid Gearing*, 1986.

Tell Us What You Think . . .
If you found these Revolutions of interest and/or useful, please circle **201**.